



**HAL**  
open science

# Enantioselective nickel catalyzed butadiene hydroalkoxylation with ethanol: from experimental results to kinetics parameters

Alexis Mifleur, Isabelle Suisse, Andre Mortreux, Mathieu Sauthier

## ► To cite this version:

Alexis Mifleur, Isabelle Suisse, Andre Mortreux, Mathieu Sauthier. Enantioselective nickel catalyzed butadiene hydroalkoxylation with ethanol: from experimental results to kinetics parameters. *Catalysis Letters*, 2020, *Catalysis Letters*, 151, pp.27-35. 10.1007/s10562-020-03267-z . hal-04272735

**HAL Id: hal-04272735**

**<https://hal.univ-lille.fr/hal-04272735>**

Submitted on 6 Nov 2023

**HAL** is a multi-disciplinary open access archive for the deposit and dissemination of scientific research documents, whether they are published or not. The documents may come from teaching and research institutions in France or abroad, or from public or private research centers.

L'archive ouverte pluridisciplinaire **HAL**, est destinée au dépôt et à la diffusion de documents scientifiques de niveau recherche, publiés ou non, émanant des établissements d'enseignement et de recherche français ou étrangers, des laboratoires publics ou privés.

1 **Enantioselective nickel catalyzed butadiene hydroalkoxylation**  
2 **with ethanol: from experimental results to kinetics parameters**

3 Alexis Mifleur, Isabelle Suisse, André Mortreux, Mathieu Sauthier\*

4 Univ. Lille, CNRS, Centrale Lille, Univ. Artois, UMR 8181 - UCCS - Unité de Catalyse et Chimie du  
5 Solide, F-59000 Lille, France

6 Dedicated to Prof. Alan Welch on the occasion of his retirement from Heriot-Watt University

7 **Abstract**

8 The enantioselective hydroalkoxylation of butadiene with ethanol has been performed in the presence of  
9 nickel-based catalysts and chiral diphosphine ligands. Ee's up to 77 % could be obtained from the use of  
10 atropisomeric chiral ligands such as Segphos. The kinetics parameters of the reaction were determined  
11 using a qualitative kinetic model to better explain the l/b isomerization and racemization processes  
12 observed for long reaction times.

13

14

15

16

17

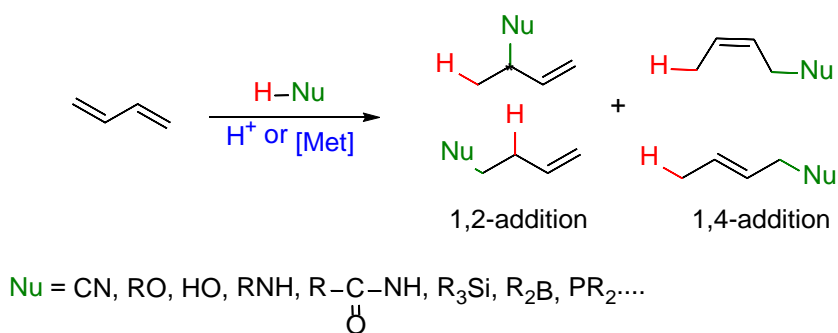
18

19

20

## 1 Introduction

2 Double bond hydrofunctionalization is one of the most fundamental reactions in organic synthesis leading  
3 to a large variety of compounds [1]. This reaction corresponds to the addition of hydrogen and another  
4 fragment across a carbon-carbon or carbon-heteroatom multiple bond and is generally promoted by a  
5 Brønsted acid or a transition metal catalyst [2-10]. From an atom-economy standpoint, this transformation  
6 is ideal with no production of wastes. With butadiene, the hydrofunctionalization reaction leads to the  
7 formation of various functionalized alkenes according to the nucleophile (Scheme 1) [11-21]. Butenyl  
8 products issued from the 1,2- or 1,4-addition are thus obtained as a mixture of several isomers: the two  
9 1,2-addition products with the Markovnikov and anti-Markovnikov compounds and the two 1,4-adducts that  
10 differ from the (*Z*) and (*E*) configurations of the internal C=C double bond.



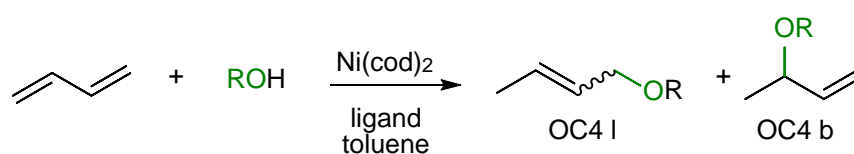
11

12

**Scheme 1.** Hydrofunctionalization of butadiene

13 Among these examples, the hydroalkoxylation is particularly attractive since this transformation using  
14 readily accessible alcohols as nucleophiles leads to the formation of allylethers via a catalytic and  
15 environmentally friendly process. This approach is on this point of view advantageous in comparison to the  
16 classical Williamson reaction ( $\text{S}_{\text{N}}2$  reaction on an allylic halide derivative) which produces high quantity of  
17 inorganic salts as co-products [22]. Nevertheless, this transformation has been relatively rarely described  
18 in the literature, unlike considering the telomerization reaction which corresponds to the dimerization of  
19 butadiene with addition of a nucleophile [23]. Various metals as rhodium [24-26], palladium [28,29], nickel  
20 [30-33] as well as aluminum [34-36] or gold [37] have been used to design suitable catalysts. In our hands,

1 the hydroalkoxylation of dienes with simple and bio-sourced alcohols has been performed in the presence  
2 of nickel precatalysts associated with chelating diphosphine ligands (Scheme 2) [14-16]. With this catalytic  
3 system, high butadiene conversions and selectivities in alkylbutenyl ethers were obtained with low catalyst  
4 loadings. The major products are the branched butenylether (OC4 b) together with the linear isomer (OC4  
5 l). The allylic structures of the branched or linear ethers formed and the absence of product issuing from  
6 the 1,2 anti-Markovnikov addition strongly support the involvement of  $\pi$ -allylnickel intermediates rather  
7 than a direct nucleophilic attack on the diene. [38]



9 **Scheme 2.** Nickel catalyzed butadiene hydroalkoxylation

10 As the branched ether bearing a stereogenic center is obtained as major isomer of the reaction, we were  
11 interested in the enantioselective version of the nickel catalyzed hydroalkoxylation reaction. This  
12 asymmetric version is relevant as it offers an access to enantiomerically enriched small building blocks.  
13 Chiral allylethers are commonly found in bioactive molecules and industrially important pharmaceutical  
14 intermediates [39]. To our knowledge, the enantioselective hydrofunctionalization of dienes with alcohols  
15 is rare with only one recent example reported in the literature [40]. Herein we report our recent progress  
16 in the enantioselective butadiene hydroalkoxylation with ethanol as model substrate.

## 17 **2 Experimental**

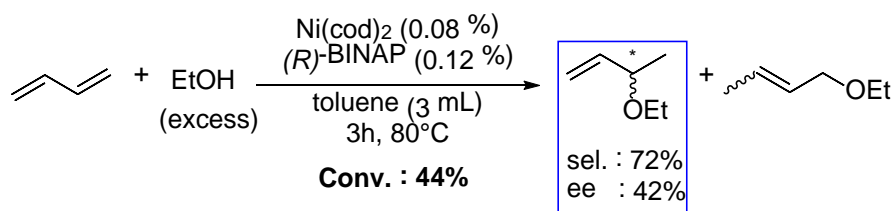
18 Chemicals were purchased from Aldrich, Alfa Aesar, Acros, Linde Gas France (butadiene) and Strem. Ethanol  
19 was distilled over magnesium turnings. Toluene was obtained from a solvent purification system MBraun  
20 SPS-800. Conversions and selectivities were determined by gas chromatography on a Shimadzu 2010  
21 apparatus equipped with an Equity-5 column (30 m, i.d. = 0.32 mm). Ee's were determined by chiral GC  
22 using a ChiralDex column with H<sub>2</sub> as gas vector.

1 *Catalytic test:* The catalytic solution is prepared in a glovebox by mixing Ni(cod)<sub>2</sub> (3.8 mg, 0.014 mmol) and  
2 the ligand (0.021 mmol) in 3 mL toluene in a glass reactor closed by a Rotaflor<sup>®</sup> stopcock. Under nitrogen  
3 atmosphere, the tube was cooled at -15 °C and dry and degassed EtOH was added (10 mL). A precise amount  
4 of butadiene (1.5 mL, 17.2 mmol) was then condensed at low temperature and transferred in the reaction  
5 mixture via a cannula. The glass reactor was closed and heated to 80°C for 30 hours. After reaction, the  
6 mixture was cooled and vented before GC analyses with heptane as internal standard. Branched vs linear  
7 products could be differentiated.

8

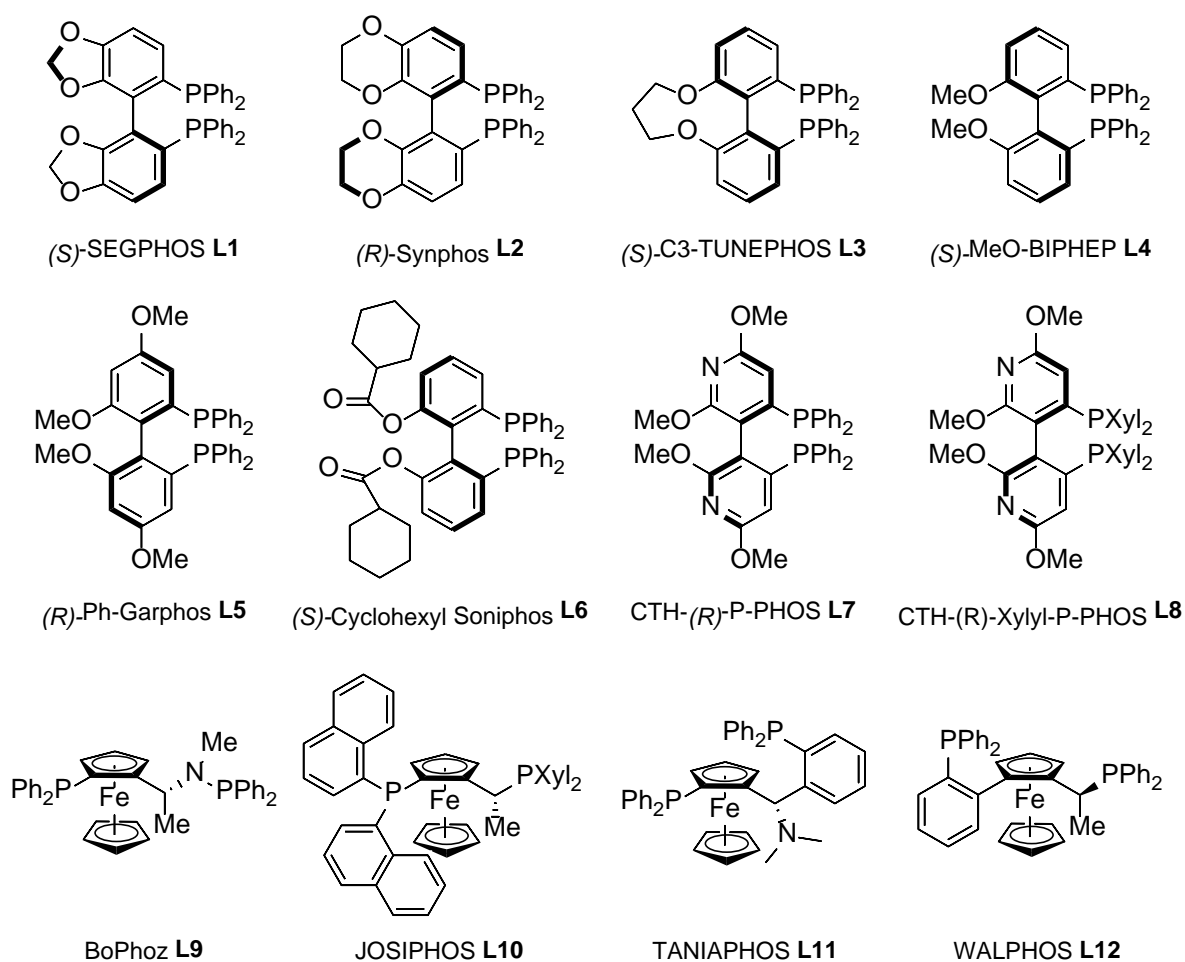
### 9 **3 Results and discussion**

10 Our group has recently reported that the hydroalkoxylation reaction can be achieved with both high  
11 butadiene conversions and high selectivities when using a catalytic system featuring zerovalent nickel in the  
12 presence of particular chelating diphosphines with two phosphorous atoms bridged with four carbons [14-  
13 16]. Among the commercially available and optically pure C<sub>4</sub> diphosphines, BINAP is one of the most  
14 representative ligands with an axial chirality. BINAP is elsewhere used in asymmetric catalytic  
15 hydrogenations on an industrial scale, particularly for the synthesis of (-)-menthol [41]. An explorative trial  
16 for butadiene hydroalkoxylation reaction with (*R*)-BINAP has been conducted and displayed a moderate  
17 conversion (44%). Nevertheless, the regioselectivity for the branched product was important (72%) and a  
18 promising enantiomeric excess has been obtained (42%) with a low catalyst loading (0.08 mol %) (Scheme  
19 3).



21 **Scheme 3.** Nickel based butadiene asymmetric hydroalkoxylation with ethanol using (*R*)-BINAP ligand

1 Thanks to this encouraging result, we screened a series of chiral ligands (**Figure 1**) for the butadiene  
 2 hydroalkoxylation with ethanol using Ni(cod)<sub>2</sub> as source of zerovalent nickel, according the standard  
 3 conditions reported for the evaluation of this catalytic system [15]. The previous procedure used with BINAP  
 4 has been reproduced: toluene was used as co-solvent to insure a good solubility of the catalyst in the  
 5 reaction media and the reactions were conducted at 80 °C. A first series of catalytic results is reported in  
 6 Table 1.



7  
 8 **Figure 1.** First series of chiral ligands used for the nickel catalyzed asymmetric hydroalkoxylation of  
 9 butadiene with ethanol

10

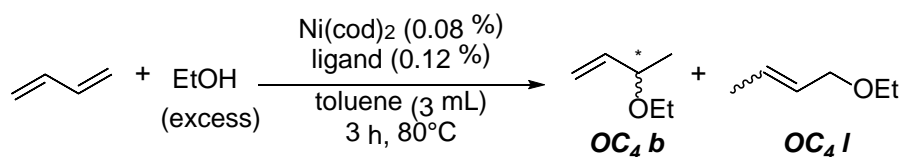
11

1

2 **Table 1.** Variation of the chiral ligand for butadiene hydroalkoxylation<sup>a</sup>

3

4



5

6

7

8

9

10

11

12

13

14

15

16

17 We initially applied ligands with an atropisomeric C<sub>2</sub>-symmetric biaryl backbone as BINAP: (*S*-18 Segphos **L1**, (*R*)-Synphos **L2**, (*S*)-C3-Tunephos **L3**, (*S*)-MeO-Biphep **L4**, (*R*)-Ph-Garphos **L5**, (*S*)-Cyclohexyl

Entry	Ligand	Conversion <sup>b</sup> (%)	Selectivity OC <sub>4</sub> b <sup>b</sup> (%)	Ee <sup>c</sup> (%)
<b>1</b>	<b>L1</b> ( <i>S</i> )-Segphos	66	71	68
<b>2<sup>d</sup></b>	<b>L1</b> ( <i>S</i> )-Segphos	31	75	77
<b>3</b>	<b>L2</b> ( <i>R</i> )-Synphos	97	64	15
<b>4</b>	<b>L3</b> ( <i>S</i> )-C3-TUNEPHOS	17	70	69
<b>5</b>	<b>L4</b> ( <i>S</i> )-MeO-BIPHEP	67	72	58
<b>6</b>	<b>L5</b> ( <i>R</i> )-Ph-Garphos	88	69	27
<b>7</b>	<b>L6</b> ( <i>S</i> )-cyclohexyl Soniphos <sup>e</sup>	33	68	63
<b>8</b>	<b>L7</b> CTH-( <i>R</i> )-P-Phos	17	74	64
<b>9</b>	<b>L8</b> CTH-( <i>R</i> )-Xylyl-P-Phos <sup>e</sup>	87	68	45
<b>10</b>	<b>L9</b> BoPhoz	94	85	13
<b>11</b>	<b>L10</b> JOSIPHOS	94	87	13
<b>12</b>	<b>L11</b> TANIAPHOS	18	91	16
<b>13</b>	<b>L12</b> WALPHOS	32	92	53

<sup>a</sup> Butadiene : 17.2 mmol, Ni(cod)<sub>2</sub> /ligand /butadiene (0,08% : 0,12% : 1), EtOH : 10 mL, toluene : 3 mL, ; T : 80°C, t : 3 hours.  
<sup>b</sup> Calculated by GC analysis, from the amount of butenyl ethers, using n-heptane as internal standard.  
<sup>c</sup> Calculated by GC analysis using a Chiraldex column  
<sup>d</sup> Reaction conducted at 60°C  
<sup>e</sup> t : 4 hours

1 Soniphos **L6**, CTH-(*R*)-P-Phos **L7** and CTH-(*R*)-Xylyl-P-Phos **L8** (entries 1-9). Yields in butenyl ethers were  
2 measured in the 17-97 % range and selectivities for the branched chiral ether varied from 64 % to 75 %.  
3 Butadiene dimers and telomers are occasionally observed as traces (up to 5%).The best combinations  
4 between yields and enantioselectivities were obtained with **L1** and **L4** (entries 1 and 5) with respectively  
5 66% yield and 68% ee for **L1** and 67% yield and 58% ee for **L4**. When the experiment was performed at  
6 lower temperature with **L1** (entry 2), 60°C instead 80°C, the yield decreased to 31% while the selectivity  
7 into the branched isomer increased as well as the enantioselectivity (75% and 77% vs 71% and 68%,  
8 respectively). Among these atropisomeric ligands, **L2** and **L5** led to the highest OC<sub>4</sub> yields, but provided low  
9 enantiomeric excesses with 15% and 27% ee respectively (Entries 3 and 6). The highest enantiomeric excess  
10 was obtained with the ligand **L3** (69% ee) along with a very low yield (17%) (Entry 4).

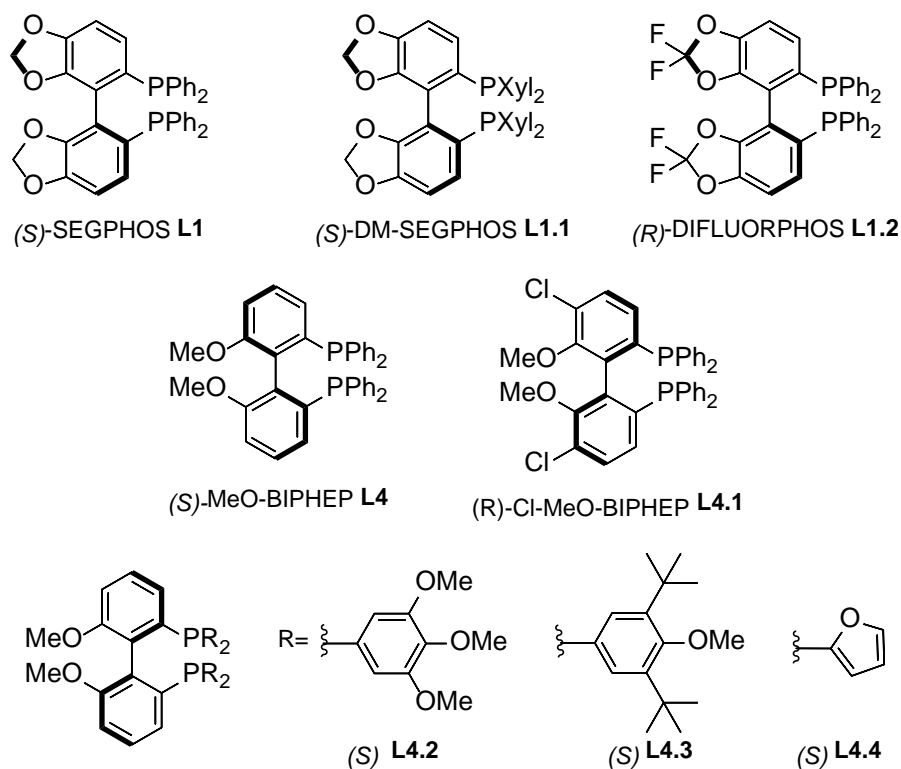
11 We next considered chiral ligands with ferrocenyl structures (**L9-L12**). A nickel catalyst bearing  
12 Bophoz **L9** or Josiphos **L10** provides high yields in butenyl ethers but with low enantiomeric excesses (94 %  
13 yield and 13 % ee) (Entries 10 and 11). A low conversion as well as a low ee are obtained with Taniaphos  
14 **L11** (Entry 12). In this series of ligands, the most interesting enantiomeric excess obtained with ferrocenyl  
15 based ligand is with Walphos **L12** with 53 % ee but with a rather low conversion (Entry 13).

16 As ligands **L1** and **L4** gave the best compromise in terms of butadiene conversions and enantiomeric  
17 excesses, variation of **L1** and **L4** structures either on their phosphorous atoms or on their backbones was  
18 considered (Figure 2). Results are reported in Table 2. The change of the phenyl substituents on  
19 phosphorous of the Segphos by electro-donating xylyl groups ((*S*)-DM-Segphos **L1.1**) (Entry 2 vs 1) improves  
20 the conversion of butadiene into butenylether to 89 % along with a rather similar enantiomeric excess  
21 (compare entries 1 and 2). On the other side, the use of (*R*)-Difluorophos **L1.2** bearing fluorine atoms in  
22 position 2 of the dioxole moieties decreases drastically both the yield in OC<sub>4</sub> as well as the enantiomeric  
23 excess (entry 3). Reaction with (*S*)-Cl-MeO-Biphep **L4.1** which bears chloro groups on 5 and 5' position  
24 displays lower yield and enantiomeric excess than **L4** (entry 5) and electron rich aryl group on the  
25 phosphorous atom such as 3,4,5-trimethoxyphenyl **L4.2** leads to similar results (compare entry 6 and entry



1 5). The use of the ligand **L4.3** with an electron-donating methoxy group and bulky *tert*iobutyl substituents  
2 on the phenyl rings increases surprisingly the conversion of butadiene into butenylether with a high  
3 selectivity for the branched isomer (95 %). Unfortunately, a moderate enantiomeric excess was obtained  
4 (21 % ee) (compare entries 4, 5 and 7). Electron poor releasing substituents at phosphorous (**L4.4**) did not  
5 allow any conversion of the diene.

6



7

8

**Figure 2.** Atropisomeric diphosphine ligands

9

10

11

12

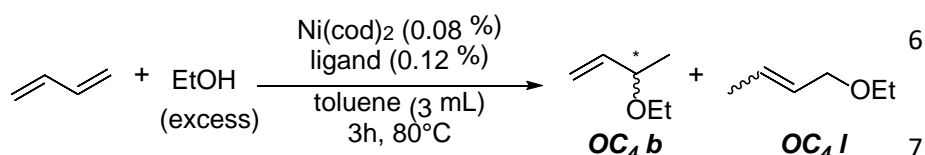
13

14

15

1  
2  
3  
4  
5

**Table 2.** Effect of Segphos and MeO-BIPHEP derivative ligands on the enantioselective butadiene hydroalkoxylation



Entry	Ligand	Conversion <sup>b</sup> (%)	Selectivity OC <sub>4</sub> b <sup>b</sup> (%)	Ee <sup>c</sup> (%)
1	L1 (S)-Segphos	66	71	68
2	L1.1 (S)-DM-Segphos	89	74	64
3	L1.2 (S)-difluorophos	7	66	48
4	L4 (S)-MeO-Biphep	67	72	58
5	L4.1 (R)-Cl-MeO-Biphep	40	71	49
6	L4.2 (S)-L4.2	42	64	50
7	L4.3 (S)-L4.3	99	95	21
8	L4.4 (S)-L4.4	0	-	-

<sup>a</sup> butadiene : 17.2 mmol, Ni(cod)<sub>2</sub>/ligand/butadiene (0,08% : 0,12% : 1), EtOH : 10 mL, toluene : 3 mL, T : 80°C, t : 3 hours.

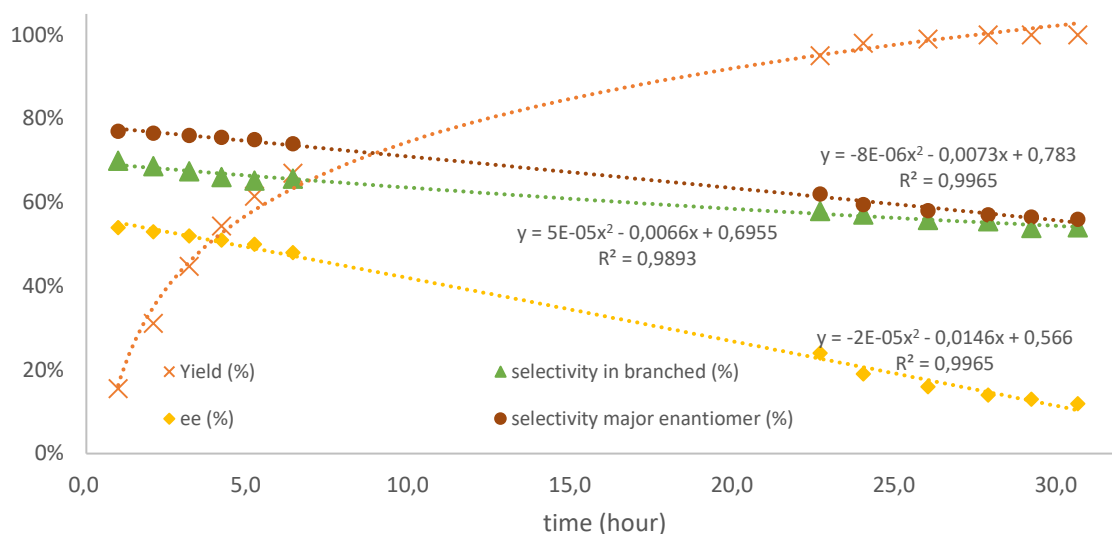
<sup>b</sup> Calculated by GC analysis, from the amount of butenyl ethers determined using n-heptane as internal standard

<sup>c</sup> Calculated by GC analysis using a Chiraldex column

15

16 Among the different catalysts used in this study, several of them displayed a high catalytic activity  
17 but led to a low enantioselectivity. This behavior suggested that undesired processes of isomerization /  
18 racemization of the different isomeric allylic ethers formed during the reaction could occur. We thus  
19 considered studying the evolution of the enantiomeric excess vs conversion on a selected example. The  
20 combination of CTH-(R)-Xylyl-P-Phos **L8** with Ni(cod)<sub>2</sub> was chosen for this study as a high yield and a  
21 moderate enantiomeric excess were obtained with this catalytic system. Standard reaction conditions were

1 used and aliquot samples of the reaction mixture were taken and analyzed by GC at regular time intervals  
 2 (Figure 3). As expected, the global yield in ethers increases rapidly at the beginning of the reaction, then  
 3 the reaction rate decreases, and the full conversion is reached after 28 hours. Besides, the butenylethers  
 4 selectivities are moving towards a thermodynamic equilibrium via an isomerization along with an  
 5 epimerization process. Firstly, the yield into the branched ether decreased regularly to the benefit of the  
 6 linear one. This phenomenon of isomerization of the branched compounds (including both enantiomers)  
 7 into the linear isomer follows a decreasing profile from 70 % to 54 %. Similarly, the major enantiomer within  
 8 the branched ethers decreases from 77 % after 30 h. Noteworthy are the values observed at 46 h, which  
 9 are respectively 53% of branched butenylethers and 54% of the major enantiomer. As expected, the  
 10 enantiomeric excess is decreasing faster.



11

12 **Figure 3.** Ethers yields, OC4 b selectivities, major enantiomer selectivities and OC4 b enantiomeric excesses  
 13 as function of time

14 (Conditions : Butadiene = 17.2 mmol, Ni(cod)<sub>2</sub>/ligand/butadiene (0,08 mol % : 0,12 mol % : 1), EtOH = 10 mL, toluene = 3 mL,  
 15 T = 80°C.)

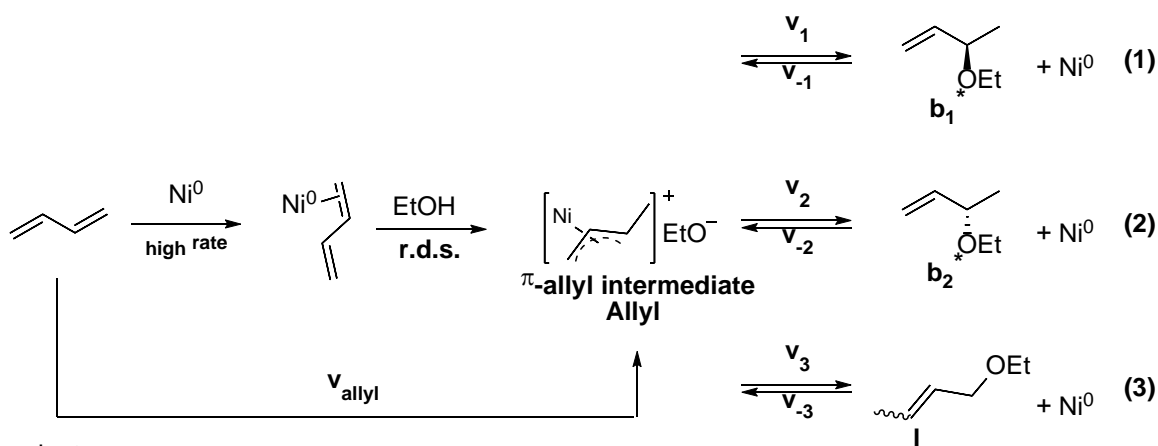
16

17 This important evolution in the products ratio implies both isomerization and racemization  
 18 processes with time. A cationic Ni-allyl complex has been proposed by our group to be the key intermediate  
 19 during the formation of butenyl ethers [38]. The computed barriers, in the case of the non-chiral ligand

1 dppb, indicated an initial kinetic preference for the formation of the branched butenyl ether product but  
 2 the low calculated energy barrier for the C-O bond formation from the nickel  $\pi$ -allyl intermediate allows  
 3 considering the reversibility of this step and the observed isomerization.

4 Herein, we propose a qualitative kinetic model based on the reactions described in Scheme 4 in  
 5 order to extract the kinetic parameters. Previous DFT calculations showed that the formation of this cationic  
 6  $\pi$ -allyl nickel is accessible by direct protonation by ethanol of the initially formed butadiene-Ni(0) complex  
 7 leading to an ion-pair featuring a Ni-allyl cation along with free ethoxide as counteranion [38]. Based on  
 8 these previous calculations, this step corresponds to the highest activation energy value of the overall  
 9 reaction. Moreover, the difficulties encountered monitoring the concentration of nickel species lead up to  
 10 simplify the kinetic model. As a consequence, the initial elementary steps: nickel-diene coordination and  $\pi$ -  
 11 allyl formation are considered as one simplified step with a rate corresponding to the RDS of this reaction,  
 12 the  $\pi$ -allyl formation. Because the ethanol is both the nucleophile of this reaction and the solvent (so used  
 13 in large excess), we applied an order degeneration simplification and thus the apparent rate constant  $k_{\text{allyl}}$   
 14 corresponds to  $k[\text{EtOH}]$ . The next elementary steps leading to the formation of the products from this  
 15 intermediate are supposed to be reversible (steps **(1)**, **(2)** and **(3)**) as suggested by the experimental results  
 16 (Figure 3, epimerization and isomerization of the butenyl ethers).

17



18  $\text{Ni}^0$ : zero-valent nickel coordinated to the bidentate ligand

19 **Scheme 4**  $\pi$ -allyl nickel intermediate and products formed during hydroalkoxylation of butadiene

$$\begin{aligned}
v_{allyl} &= k_{allyl}[but][Ni^0] \\
v_1 &= k_1[Allyl] \\
v_{-1} &= k_{-1}[b_1^*][Ni^0] \\
v_2 &= k_2[Allyl] \\
v_{-2} &= k_{-2}[b_2^*][Ni^0] \\
v_3 &= k_3[Allyl] \\
v_{-3} &= k_{-3}[l][Ni^0]
\end{aligned}
\tag{4}$$

$$\begin{aligned}
\frac{d[But]}{dt} &= -v_{allyl} \\
\frac{d[Ni^0]}{dt} &= -v_{allyl} + v_1 - v_{-1} + v_2 - v_{-2} + v_3 - v_{-3} \\
\frac{d[Allyl]}{dt} &= v_{allyl} - v_1 + v_{-1} - v_2 + v_{-2} - v_3 + v_{-3} \\
\frac{d[b_1^*]}{dt} &= v_1 - v_{-1} \\
\frac{d[b_2^*]}{dt} &= v_2 - v_{-2} \\
\frac{d[l]}{dt} &= v_3 - v_{-3}
\end{aligned}
\tag{5}$$

**Figure 4** : Proposed kinetic model

1 Next, the kinetic constants for the other elementary steps were estimated at 353 K by minimizing  
2 the least squares with the solver displays by Microsoft Excel® and the GRG (Generalized Reduced Gradient)  
3 non-linear solving method. A multistart with 100 samples sized population was preferred to limit local  
4 minima in our estimation.

5 Values of the kinetic parameters are reported in Table 3. Rate constants  $k_1$ ,  $k_2$  and  $k_3$  display values  
6 between 5.9 and 18.8  $\text{min}^{-1}$  with  $k_1 > k_3 > k_2$ . Contrariwise, the rate constants for the reverse ways are in  
7 different orders of magnitude, with values included between  $10^{-5}$  and  $10^{-1}$   $\text{L.mol}^{-1}.\text{min}^{-1}$  following the same  
8 order than the direct way. The significant differences between the values obtained for the direct and indirect  
9 ways show that the formation of the butenylethers are fostered vs the formation of the allylic intermediate.  
10 The model accuracy is very good as illustrated by the parity plot of Figure 4.

11 **Table 3** Optimal parameters of the kinetic model<sup>a</sup>

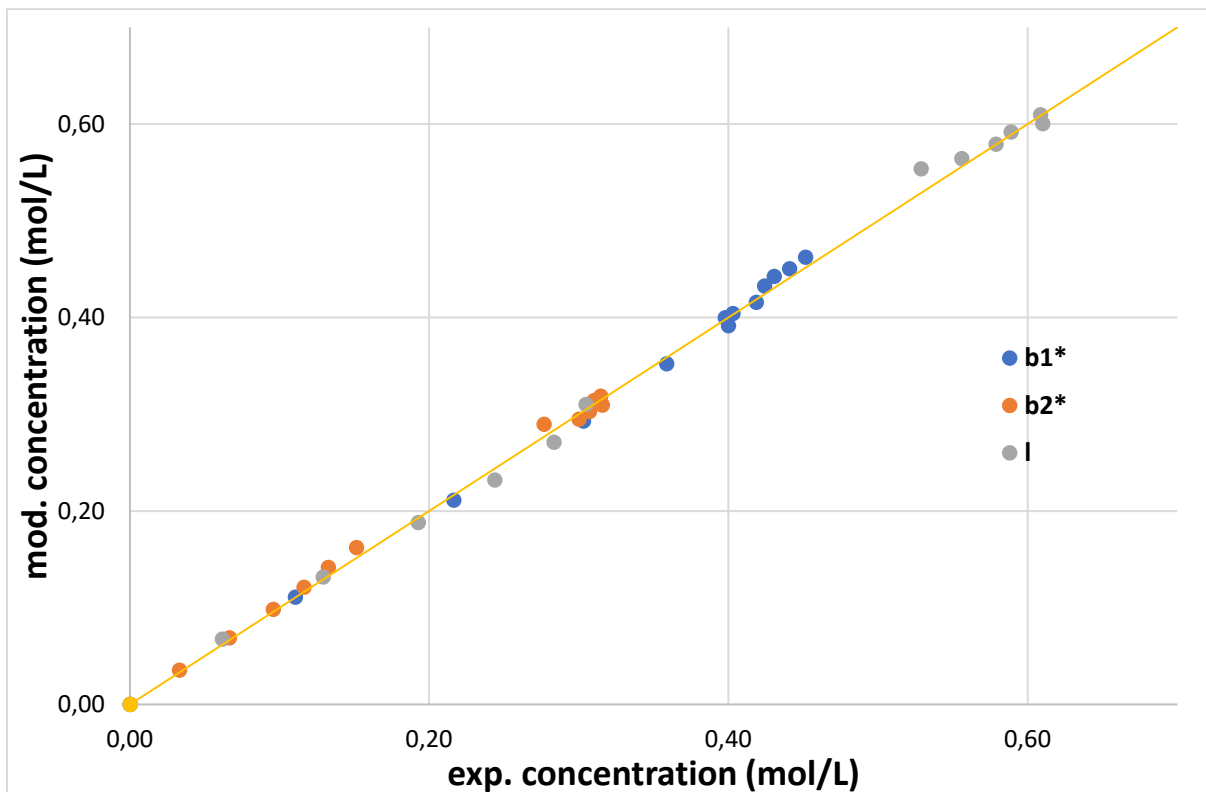
$k_{allyl}$ ( $\text{L.mol}^{-1}.\text{min}^{-1}$ )	$k_1$ ( $\text{min}^{-1}$ )	$k_{-1}$ ( $\text{L.mol}^{-1}.\text{min}^{-1}$ )	$k_2$ ( $\text{min}^{-1}$ )	$k_{-2}$ ( $\text{L.mol}^{-1}.\text{min}^{-1}$ )	$k_3$ ( $\text{min}^{-1}$ )	$k_{-3}$ ( $\text{L.mol}^{-1}.\text{min}^{-1}$ )
3.3	18.8	$7.7 \cdot 10^{-1}$	5.9	$6.0 \cdot 10^{-5}$	11.2	$4.0 \cdot 10^{-4}$

	$K_1 = 24^c$	$K_2 = 97550^c$	$K_3 = 27351^c$
--	--------------	-----------------	-----------------

<sup>a</sup> estimated at 353 K

<sup>b</sup>  $k_{allyl} = k_{app} = k[EtOH]$

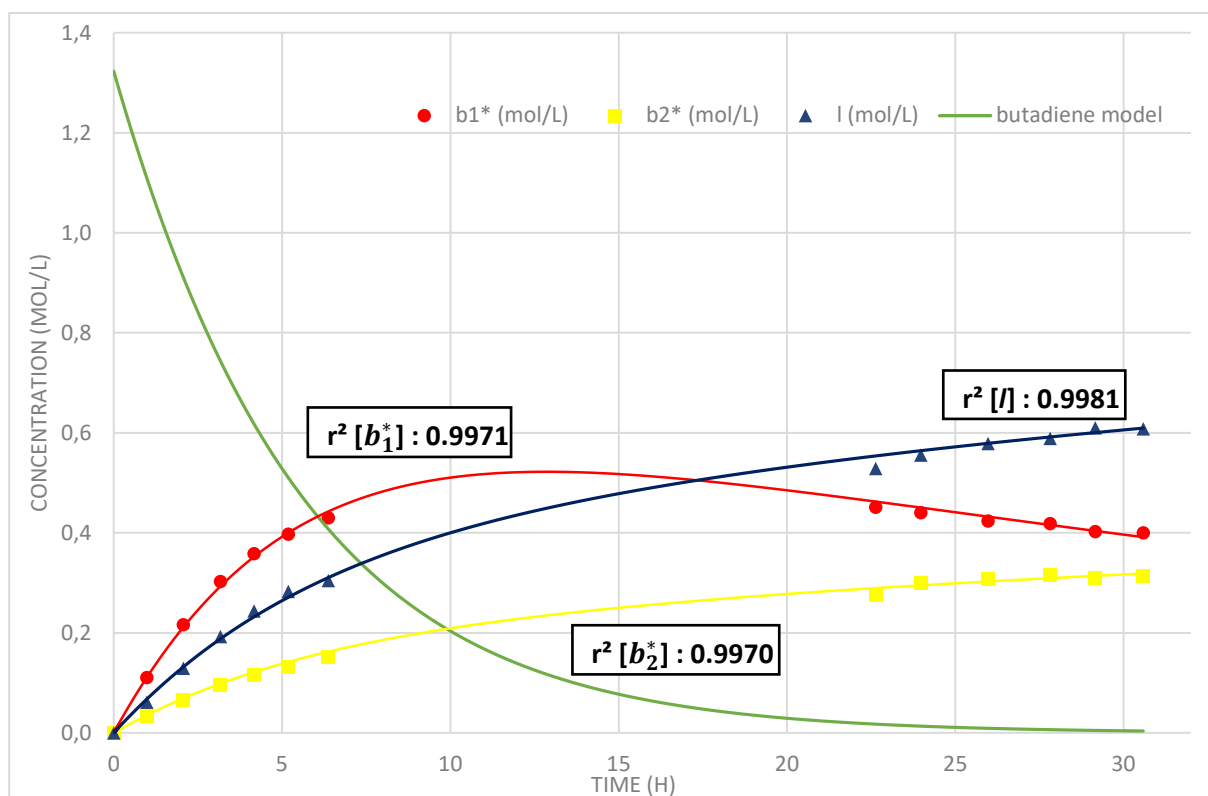
<sup>c</sup>  $K_x = k_x / k_{-x}$



1

2 **Figure 4** Parity plot of model concentration vs experimental concentration

3 Analysis of the experimental data at the early stage, before that the isomerization and racemization  
4 processes get a significant impact on the rate law of the reaction, may help in validating this computational  
5 approach. As an apparent zero order applies until a c.a. 30 % conversion, an average rate corresponding to  
6 the initial rate determining step allyl complex formation is obtained. This experimental value  $v_0 = k_{app}$  is  
7 found to be  $3.3 \text{ L}\cdot\text{mol}^{-1}\cdot\text{min}^{-1}$  with  $k_{app}$  including the ethanol concentration. Both values, obtained from  
8 computational approach and experimentally are concurring exactly.



1

2

**Figure 6** Experimental and simulated concentrations of products with time.

3

Experimental and simulated concentrations of products with time are reported in Figure 6. It

4

appears that  $b_1^*$  as kinetic product is preferentially formed at the beginning of the reaction while the rates

5

of formation of  $b_2^*$  and  $I$  are lower, but their selectivities increase regularly vs conversion. As the butadiene

6

concentration decreases, the  $\pi$ -allyl complex intermediate resulting from the oxidative addition of the

7

butenylethers on a low valent Ni(0) species ( $k_{-1}$ ,  $k_{-2}$ ,  $k_{-3}$ ) still remains the key species of the isomerization

8

and epimerization processes. The affinity of the products with the chiral nickel complex illustrates the

9

differences observed between the kinetic parameters. One can expect that the spatial configuration of the

10

enantiomer  $b_1^*$  allows for its preferable interaction with the chiral catalyst according to a "lock and key"

11

molecular recognition as opposed to the other enantiomer  $b_2^*$  and the linear ether  $I$  [42]. As a result, the

12

rate of the reverse way for the elementary step **(1)** is much higher than the ones for **(2)** and **(3)**. This way

13

back of  $b_1^*$  to produce the allylic nickel intermediate tends this major enantiomer to be gradually consumed

14

while its opposite enantiomer  $b_2^*$  and the linear isomer  $I$  accumulate in the reaction mixture.

1           Equilibrium constants determined for the elementary steps of products formation from the allylic  
2 intermediate are superior to 1 and confirm the predominance of the direct ways against the reverse  
3 reactions. As expected from the higher decreasing rate of the ee vs *the* isomerization,  $K_1$  is the lowest  
4 equilibrium constant among these steps for the butenylethers formation and equilibration.  $K_2$  and  $K_3$  are  
5 respectively 4000 and 1100 times higher.

## 6 **Conclusion**

7 In conclusion, nickel catalyzed asymmetric hydroalkoxylation of butadiene with ethanol has been  
8 successfully performed in the presence of chiral diphosphine ligands. Enantiomeric excesses up to 77 %  
9 have been obtained with high yields. Nonetheless, the chemo- and enantioselectivity of the reaction are  
10 governed by the kinetic of the reaction: at the initial stage, the kinetic enantiomer is observed as the major  
11 isomer leading to high chemo- and enantioselectivities. Then, the enantiomeric excess and the selectivity  
12 into the branched isomer decrease with time due to racemization and isomerization reactions. Although  
13 higher enantiomeric excesses are obtained for short reaction time and are decreasing gradually, this  
14 catalytic system is very easy to carry out and can be considered as an interesting tool for the asymmetric  
15 synthesis of chiral allylic ethers. Further investigations are carried out in order to further increase the ee  
16 and to apply this new methodology to the synthesis of other chiral allylic ethers.

17

## 18 **Acknowledgments**

19 We are grateful to the Region Nord-Pas de Calais for A.M.'s fellowship. We acknowledge the Ministry of  
20 Research and Technology, the Institut Universitaire de France, the ANR (project H2CAT: ANR-15-CE07-0018-  
21 01) and the CNRS for their financial support. We would like to extend our gratitude to Dr Léo Violet and Dr  
22 Carole Mutschler for their precious advices.

## 23 **References**



- 1 [1] a) M. Beller, C. Bolm, *Transition Metals for Organic Synthesis: Building Blocks and Fine*  
2 *Chemicals, Second Revised and Enlarged Edition* (Wiley, 2004); b) Zeng X (2013) Recent advances  
3 in catalytic sequential reactions involving hydroelement addition to carbon-carbon multiple  
4 bonds. *Chem Rev* 113:68646–6900.
- 5 [2] a) Adamson NJ, Malcolmson SJ (2020) Catalytic enantio- and regioselective addition of  
6 nucleophiles in the intermolecular hydrofunctionalization of 1,3-dienes. *ACS Catal* 10:1060–  
7 1076; b) Long J, Wang P, Wang W, Li Y, Yin G (2019) Nickel/Brønsted acid-catalyzed chemo- and  
8 enantioselective intermolecular hydroamination of conjugated dienes. *iScience* 22:369–379.
- 9 [3] Bezenine-Lafollee S, Gil R, Prim D, Hannedouche J (2017) First-row late transition metals for  
10 catalytic alkene hydrofunctionalisation: recent advances in C-N, C-O and C-P bond formation.  
11 *Molecules* 22:1901/1–1901/29.
- 12 [4] Greenhalgh MD, Jones AS, Thomas SP (2015) Iron-Catalysed hydrofunctionalisation of alkenes  
13 and alkynes. *ChemCatChem* 7:190–222.
- 14 [5] Yadav JS, Antony A, Rao TS, Subba R, Basi V (2011) Recent progress in transition metal  
15 catalysed hydrofunctionalisation of less activated olefins. *J Organomet Chem* 696:16–36.
- 16 [6] Margrey KA, Nicewicz DA (2016) A general approach to catalytic alkene anti-Markovnikov  
17 hydrofunctionalization reactions via acridinium photoredox catalysis. *Acc Chem Res* 49:1997–  
18 2006.
- 19 [7] Liu C, Bender CF, Han X, Widenhoefer RA (2007) Platinum-catalyzed hydrofunctionalization of  
20 unactivated alkenes with carbon, nitrogen and oxygen nucleophiles. *Chem Commun* 35:3607–  
21 3618.
- 22 [8] Obligacion JV, Chirik PJ (2018) Earth-abundant transition metal catalysts for alkene  
23 hydrosilylation and hydroboration. *Nat Rev Chem* 2:15–34.
- 24 [9] Chen J, Lu Z (2018) Asymmetric hydrofunctionalization of minimally functionalized alkenes *via*  
25 earth abundant transition metal catalysis. *Org Chem Front* 5:260–272.
- 26 [10] Ananikov VP, Tanaka MT (2013) *Topics in Organometallic Chemistry* 43, Ed Springer.
- 27 [11] Hermann N, Vogelsang D, Behr A, Seidensticker T (2018) Homogeneously catalyzed 1,3-diene  
28 functionalization – A success story from laboratory to miniplant scale. *ChemCatChem* 10:5342–  
29 4365.
- 30 [12] Hydrosilylation : Ibrahim AD, Entsminger SW, Zhu L, Fout AR (2016) A highly chemoselective  
31 cobalt catalyst for the hydrosilylation of alkenes using tertiary silanes and hydrosiloxanes. *ACS*  
32 *Catal* 6:3589–3593.
- 33 [13] Hydrocyanation : Bini L, Müller C, Vogt D (2010) Ligand development in the Ni-catalyzed  
34 hydrocyanation of alkenes. *Chem Commun* 46:8325–8334.
- 35 [14] Hydroalkoxylation : Mifleur A, Mortreux A, Suisse I, Sauthier M (2017) Synthesis of C4 chain  
36 glyceryl ethers via nickel-catalyzed butadiene hydroalkoxylation reaction. *J Mol Catal A : Chem*  
37 427:25–30.
- 38 [15] Mifleur A, Ledru H, Lopes A, Suisse I, Mortreux A, Sauthier M. (2016) Synthesis of short-chain  
39 alkenyl ethers from primary and bio-sourced alcohols via the nickel-catalyzed hydroalkoxylation  
40 reaction of butadiene and derivatives. *Adv Synth Catal* 358:110-121.

- 1 [16] Bigot S, Ibn El Alami MS, Mifleur A, Castanet Y, Suisse I, Mortreux A, Sauthier M (2013) Nickel-  
2 catalysed hydroalkoxylation reaction of 1,3-butadiene: ligand controlled selectivity for the  
3 efficient and atom-economical synthesis of alkylbutenyl ethers. *Chem Eur J* 19:9785–9788.
- 4 [17] Hydrophosphinylation : Nie SZ, Davison RT, Vy MD (2018) Enantioselective coupling of dienes  
5 and phosphine oxides. *J Am Chem Soc* 140:16450–16454.
- 6 [18] Hydrophosphorylation : Mirzaei F, Han L, Tanaka M (2001) Palladium-catalyzed  
7 hydrophosphorylation of 1, 3-dienes leading to allylphosphonates. *Tetrahedron Lett* 42:297–299.
- 8 [19] Hydroamination: a) Banerjee D, Junge K, Beller M (2014) Palladium-catalysed regioselective  
9 hydroamination of 1,3-dienes: synthesis of allylic amines. *Org Chem Front* 1:368–372; b)  
10 Goldfogel MJ, Roberts CC, Meek SJ (2014) Intermolecular hydroamination of 1,3-dienes catalyzed  
11 by bis(phosphine)carbodicyclobutane-rhodium complexes. *J Am Chem Soc* 136:6227–6230; c) Yang  
12 XH, Lu A, Dong VM (2017) Intermolecular hydroamination of 1,3-dienes to generate homoallylic  
13 amine. *J Am Chem Soc* 139:14049–14052; d) Yang XH, Dong VM (2017) Rhodium-catalyzed  
14 hydrofunctionalization: enantioselective coupling of indolines and 1, 3-dienes. *J Am Chem Soc*  
15 139:1774–1777.
- 16 [20] Hydroamidation: Banerjee D, Junge K, Beller M (2014) A general catalytic hydroamidation of  
17 1,3-dienes: atom-efficient synthesis of N-allyl heterocycles, amides and sulfonamides. *Angew*  
18 *Chem Int Ed* 53:1630–1635.
- 19 [21] Hydroboration: Satoh M, Nomoto Y, Miyaura N, Suzuki A (1989) New convenient approach  
20 to the preparation of (Z)-allylic boronates via catalytic 1, 4-hydroboration of 1, 3-dienes with  
21 catecholborane. *Tetrahedron Lett* 30:3789–3792.
- 22 [22] Trost BM (1995) Atom economy—a challenge for organic synthesis: homogeneous catalysis  
23 leads the way. *Angew Chem Int Ed* 34:259–281.
- 24 [23] Fassbach TA, Vorholt AJ, Leitner W (2019) The telomerization of 1, 3-dienes—A reaction grows  
25 up. *ChemCatChem* 11:1153–1166.
- 26 [24] Dewhirst KC (1967) Reaction of rhodium trichloride with dienes. *J Org Chem* 32:1297–1300.
- 27 [25] Kawazura H, Ohmori T. (1972) On the catalytic addition of alcohols to 1, 3-butadiene with  
28 rhodium trichloride hydrates. *Bull Chem Soc Jpn* 45:2213–2214.
- 29 [26] Kawazura H, Takagaki T, Ishii Y (1975) The regioselective addition of alcohols to isoprene  
30 with rhodium trichloride hydrates. *Bull Chem Soc Jpn* 48:1949–1950.
- 31 [27] Fache E, Mercier C (1993) Addition of alcohols to isoprene catalyzed by hydrated rhodium  
32 trichloride: a way to improve the 1, 4-addition regioselectivity. *J Mol Catal* 78:21–30.
- 33 [28] Patrini R, Lami M, Marchionna M, Benvenuti F, Galletti AMR, Sbrana G (1998) Selective  
34 synthesis of octadienyl and butenyl ethers via reaction of 1, 3-butadiene with alcohols catalyzed  
35 by homogeneous palladium complexes. *J Mol Catal* 129 (2-3):179–189.
- 36 [29] Utsunomiya M, Kawatsura M, Hartwig JF (2003) Palladium-catalyzed equilibrium addition of  
37 acidic OH groups across dienes. *Angew Chem Int Ed* 42:5865–5868.

- 1 [30] Shields TC, Walker WE (1971) Nickel-complex catalyzed telomerisation of butadiene with  
2 alcohols. *J Chem Soc D* 193–194.
- 3 [31] Weigert FJ, Drinkard WC (1973) The Ni(0)-catalyzed addition of phenol to butadiene. *J Org*  
4 *Chem* 38:335–337.
- 5 [32] Beger J, Duschek C, Füllbier H, Gaube W (1974) Diene oligomerization. IX. Nickel complex-  
6 catalyzed dimerization and telomerization of butadiene in hydroxy group-containing media. *J Prakt*  
7 *Chem* 316:26–42.
- 8 [33] Commereuc D, Chauvin Y. (1974) Telomerization of butadiene with methanol using  
9 homogeneous catalysts of palladium and nickel. *Bull Soc Chim Fr* 3-4:652–656.
- 10 [34] Boelens H, Ter Heide R, Rijkens F (1968) Chemical structure and odor. VI. Geraniol derivatives.  
11 *Am Perfum Cosmet* 83:27–30.
- 12 [35] Behr A, Johnen L, Neubert P (2012) A sustainable route from the renewable myrcene to methyl  
13 ethers via direct hydroalkoxylation. *Catal Sci Technol* 2:88–92.
- 14 [36] Williams DBG, Sibiya MS, Van Heerden PS (2012) Efficient hydroalkoxylation of alkenes to  
15 generate octane-boosting ethers using recyclable metal triflates and highly active metal  
16 triflate/Brønsted acid-assisted catalysts. *Fuel Process Technol* 94:75–79.
- 17 [37] Chandrasekhar B, Ryu JS (2012) Gold-catalyzed intramolecular hydroalkoxylation/cyclization  
18 of conjugated dienyl alcohols. *Tetrahedron* 68:4805–4812.
- 19 [38] Mifleur A, Mérel D, Mortreux A, Suisse I, Capet F, Trivelli X, Sauthier M, MacGregor SA (2017)  
20 Deciphering the mechanism of the nickel-catalyzed hydroalkoxylation reaction: a combined  
21 experimental and computational Study. *ACS Catal* 7:6915–6923.
- 22 [39] Trost BM, Crawley ML (2003) Asymmetric transition-metal-catalyzed allylic alkylations:  
23 applications in total synthesis. *Chem Rev* 103:2921–2943.
- 24 [40] Tran G, Mazet C (2019) Ni-catalyzed regioselective hydroalkoxylation of branched 1,3-dienes.  
25 *Org Lett* 21:9124–9127.  
26
- 27 [41] Kumobayashi H, Miura T, Sayo N, Saito T, Zhang X (2001) Recent advances of BINAP chemistry  
28 in the industrial aspects. *Synlett* 1055–1064.
- 29 [42] Trost BM, Van Vranken DL (1992) Asymmetric ligands for transition metal catalyzed reactions:  
30 2-diphenylphosphinobenzoyl derivatives of C2 symmetrical diols and diamines. *Angew Chem Int*  
31 *Ed* 31:228–230.
- 32
- 33
- 34